# Lin28a regulates neuronal differentiation and controls miR-9 production

**Jakub S. Nowak**[1], **Nila Roy Choudhury**[1], **Flavia de Lima Alves**[1], **Juri Rappsilber**[1,2], and **Gracjan Michlewski**[1,3]

[1]Wellcome Trust Centre for Cell Biology, University of Edinburgh, King's Buildings, Edinburgh EH9 3JR, UK

[2]Department of Biotechnology, Technische Universität Berlin, 13353 Berlin, Germany

## Abstract

microRNAs shape the identity and function of cells by regulating gene expression. It is known that brain-specific miR-9 is controlled transcriptionally; however, it is unknown whether post-transcriptional processes contribute to establishing its levels. Here, we show that miR-9 is regulated transcriptionally and post-transcriptionally during neuronal differentiation of the embryonic carcinoma cell line P19. We demonstrate that miR-9 is more efficiently processed in differentiated than undifferentiated cells. We reveal that Lin28a affects miR-9 by inducing the degradation of its precursor through a uridylation-independent mechanism. Furthermore, we show that constitutively expressed untagged but not GFP-tagged Lin28a decreases differentiation capacity of P19 cells, which coincides with reduced miR-9 levels. Finally, using an inducible system we demonstrate that Lin28a can also reduce miR-9 levels in differentiated P19 cells. Together, our results shed light on the role of Lin28a in neuronal differentiation and increase our understanding of the mechanisms regulating the level of brain-specific microRNAs.

## Keywords

miRNA biogenesis; neuronal differentiation, brain-specific microRNAs; RNP complex; Lin28a

Small (21-22 nt) RNAs called microRNAs (miRs) have emerged as vital regulators of the post-transcriptional control of gene expression[1]. The maturation pathway of microRNAs, involving nuclear cleavage by the Drosha/DGCR8 complex and cytoplasmic processing by the Dicer complex, has been well described and reviewed[2,3]. A mature microRNA, upon entering the microRNA-induced silencing complex (miRISC), partially base pairs with target mRNA, exerting translational repression and/or mRNA degradation[4-6]. A number of

microRNAs are expressed in a tissue-specific, differentiation or developmental-stage specific manner, thereby contributing to cell identity and function[7]. Importantly, misregulation of microRNA levels is associated with many pathological conditions, resulting in over or under-inhibition of disease-associated genes[8-11]. Regulation of cellular microRNA levels is achieved by adjusting their transcription or by modulating post-transcriptional processing events[12,13]. However, the contribution of post-transcriptional control to the establishment of the levels of transcriptionally regulated microRNAs is largely unknown.

The human nervous system expresses approximately 70% of the known microRNAs, and some of these are specific to neurons[14]. It has been demonstrated that brain-specific miR-9 and miR-124 play an important role in neuronal development[15,16]. The expression of miR-9 and miR-124 is transcriptionally regulated by the RE1-silencing transcriptional factor (REST)[17,18]. Furthermore, cAMP-response element binding protein (CREB) has been shown to promote miR-9 expression[17]. miR-9 is evolutionarily conserved at the nucleotide level but its expression profile and functions are diverse within the nervous system of different species[19]. This microRNA was shown to interfere with the fibroblast growth factor 8 (Fgf8)[19] signaling cascade, an important pathway for neural plate patterning and development of the midbrain-hindbrain boundary[20]. Interestingly, it has been proposed that miR-9 regulates neurogenesis of the mouse telencephalon by orchestrating adjustments in a network of transcription factors[21]. Finally, miR-9 and miR-124 alone can transform adult fibroblasts into neurons, demonstrating their roles as master regulators of neuronal development[22].

We have previously shown that hnRNP A1, a protein implicated in many aspects of RNA processing, binds to the conserved terminal loops (CTLs) of miR-18a[23,24] and let-7a-1[25], stimulating and inhibiting processing, respectively. Furthermore, we have identified a number of other primary microRNA transcripts (including neuro-specific miR-9) with highly conserved terminal loops and hypothesized that this may reflect their requirement for auxiliary factors to regulate their processing[24,26,27]. Recently, we have demonstrated that the brain-enriched expression of miR-7, which is processed from a ubiquitous primary transcript, is supported by inhibition of its biogenesis in non-neural cells[28]. This inhibition is achieved through the HuR-mediated binding of MSI2 to the CTL of the miR-7 primary transcript. The regulation of pri- and pre-let-7 processing by the pluripotency factor Lin28 is an another example of post-transcriptional control of microRNA levels[29]. It has been well demonstrated that the binding of Lin28a to pre-let-7 induces 3′-terminal uridylation through recruitment of the TUT4 polymerase[30]. This blocks Dicer processing and induces the DIS3L2-mediated degradation of aberrantly processed pre-let-7 transcripts[31]. A number of other microRNAs have been shown to be under post-transcriptional control[32].

Here, we present evidence that the brain-specific microRNAs miR-9 is regulated not only at the transcriptional level but also post-transcriptionally. We demonstrate that Lin28a, a protein previously implicated in the regulation of let-7 biogenesis, binds to the miR-9 precursor and decreases the cellular levels of miR-9 during retinoic acid-mediated P19 cell neuronal differentiation. We show that the constitutive expression of untagged but not GFP-tagged Lin28a causes a severe differentiation phenotype by reducing the size of embryonic

bodies. Importantly, the constitutive expression of GFP-tagged Lin28a reduces the levels of let-7a but not miR-9, whereas untagged Lin28 inhibits both miR-9 and let-7a. We reveal that Lin28a controls miR-9 levels by a uridylation-independent mechanism. Finally, using an inducible Tet-On 3G system we demonstrate that Lin28a can also reduce miR-9 levels in differentiated cells. Our results provide the basis for better understanding the mechanism regulating the levels of brain-specific microRNAs and their control of neuronal differentiation.

## RESULTS

### miR-9 is controlled transcriptionally and post-transcriptionally

To determine whether post-transcriptional regulation of brain-specific miR-9 contributes to establishing its intercellular concentrations, we analyzed the level of mature and corresponding primary transcripts at different stages of P19 cell neuronal differentiation. Throughout differentiation, we observed a steady increase in the miR-9 levels to approximately 50-60-fold on days 4 and 5, reaching approximately 500-550-fold between days 8 and 10 (Fig. 1a). Importantly, the increase in primary miR-9 transcripts was higher at these time points (Fig. 1b). On day 4, we observed an approximate 520-fold increase in pri-miR-9-2, whereas on day 8, pri-miR-9-1, -2 and -3 were induced by approximately 400-, 1300- and 260-fold, respectively (Fig. 1b). A gradual increase in let-7 and rapid decrease in miR-302a (Fig. 1c, d) together with a decrease in Lin28 protein and an increase in the neuronal markers Tuj1 and GFAP (Supplementary Fig. 1a) validated an efficient neuronal differentiation phenotype. Northern blot analysis of miR-9, let-7a and miR-302a confirmed their abundance at selected stages of P19 cell neuronal differentiation (Supplementary Fig. 1b). Crucially, an unbiased RNAseq and small RNAseq analysis of undifferentiated (day 0) and differentiating (day 4) P19 cells revealed that while primary miR-9-2 levels accumulate from undetectable in d0 to ~900 of normalized reads in d4, the mature miR-9 accumulates very modestly to ~4 normalized reads in d4 (Supplementary Fig. 2). This is in stark contrast with another microRNA, which is rapidly induced upon Retinoic Acid treatment – miR-10a. Primary levels of miR-10a accumulate from undetectable in d0 to ~170 normalized reads in d4. Unlike miR-9 the levels of miR-10a increase from ~4 normalized reads in d0 to ~460 normalized reads in d4 (Supplementary Fig. 2). The levels of control primary and mature miR-16 are much more stable during differentiation. This example clearly demonstrates that miR-9 processing is repressed post-transcriptionally during early stage of neuronal differentiation, whereas miR-10a is most likely free from post-transcriptional regulation. Altogether, these results show that the accumulation of brain-specific miR-9 does not linearly correspond with the changing levels in their primary transcripts. This result suggests the existence of additional post-transcriptional mechanisms regulating the abundance of brain-specific microRNAs.

### miR-9 processing is regulated during neuronal differentiation

To determine whether the biogenesis of brain-specific miR-9 is regulated during neuronal differentiation, we employed *in vitro* processing assays. We observed an accumulation of pre-miR-9-1 and pre-let-7a in pri-microRNA processing performed in extracts from differentiated cells when compared with those from undifferentiated cells (Fig. 2).

Conversely, the processing of pri-miR-302a was more efficient in d0 than in d9 extracts, whereas the *in vitro* cleavage pattern of pri-miR-101 was more uniform throughout differentiation (Fig. 2). This result suggests that miR-9 processing is regulated by negative or positive factors in undifferentiated and differentiated P19 cells, respectively. Abolished pri-miR-9-1 and pri-let-7a-1 processing in Drosha or DGCR8-depleted HeLa cell extracts confirmed the specificity of the reactions and the molecular weights of the corresponding microRNA precursors (Supplementary Fig. 3). Interestingly, we observed nonspecific *in vitro* processing products in d0 extracts for pri-miR-9-1 (Fig. 2) that did not correspond to pre-miRs because they were not detected in processing reactions performed in d9 P19 or HeLa cell extracts (Fig. 2 and Supplementary Fig. 3). Hence, we assumed that the differentiation stage-specific accumulation of pre-miR-9-1 might arise from the regulation of Drosha cleavage or the control of their stability. Together, these observations corroborate our mature microRNA and pri-microRNA profiling results, indicating that during neuronal differentiation, the processing of brain-specific miR-9 is regulated at the post-transcriptional level.

### Lin28a is a potential regulator of miR-9 biogenesis

Conserved Terminal Loops (CTLs) have been implicated in the regulation of miR biogenesis, and miR-9 has highly conserved terminal loop[24]. Thus, we hypothesized that miR-9 CTLs might be involved in the regulation of its processing during neuronal differentiation. To find the putative regulators of miR-9 biogenesis, we used SILAC combined with RNA pull-down and Mass Spectrometry (Fig. 3a). miR-9 CTL was used to precipitate proteins from extracts derived from undifferentiated (d0) or differentiated (d9) P19 cells that were cultured with heavy [13C]Arg/[13C]Lys or light [12C]Arg/[12Lys] isotopes, respectively.

SILAC combined with RNA pull-down and Mass Spectrometry analysis revealed several proteins specifically interacting with miR-9 CTL (Fig. 3b and Supplementary Dataset 1). Our attention was drawn to the Lin28a protein, a factor implicated in the regulation of let-7 biogenesis, which was highly enriched in pull-downs from undifferentiated cells (17- and 11-fold for the miR-9 and miR-124-1 CTLs, respectively) (Fig. 3b). We validated the strong interaction between Lin28a and the miR-9-1 CTL (Fig. 3c). Crucially, this interaction was observed only in extracts derived from undifferentiated cells. In contrast, the Msi1 protein was found to predominantly interact with the miR-9-1 CTL in differentiated extracts (Fig. 3c). The observed interactions were specific because neither Lin28 nor Msi1 interacted with beads alone. Moreover, hnRNPA1, which is a ubiquitous RNA binding protein, was found to interact equally with corresponding CTLs on days 0 and 9. Indeed, the majority of the identified proteins did not show a differentiation-regulated expression. This however does not preclude their potential roles in regulating miR-9 biogenesis. Because Lin28a is a potent inhibitor of let-7 biogenesis, we hypothesized that it can also function in the regulation of brain-specific microRNA biogenesis.

To further confirm the interactions, we performed SILAC combined with pre-microRNA pull-down and Mass Spectrometry using extracts from undifferentiated P19 cells. Pre-let-7a pull-down identified Lin28a as well as Khsrp and hnRNP A1, proteins previously implicated

in the regulation of let-7 biogenesis[25,33,34] (Supplementary Table 1 and Supplementary Dataset 2). Surprisingly, we did not find TuT4 in the pre-let-7a pull-down, suggesting that the Lin28a/TuT4 interaction might be transient under our experimental conditions (Supplementary Dataset 2). Full-length pre-miR-9-1 and pre-miR-9-2 pulled down Lin28 with fold enrichment similar to that observed for pre-let-7a. The pre-miR-9 pull-down revealed a number of other specific factors that may contribute to the regulation of miR-9 processing.

To validate Lin28a binding specificity we performed RNA pull down followed by western blot analysis with a panel of pre-microRNAs. Pre-miR-9-1, pre-let-7a-1 and pre-miR-101 displayed efficient Lin28a binding (Fig. 4a). Importantly, pre-miR-16 as well as pre-miR-9-1 with substituted TL from the miR-16 (pre-miR-9-1/miR-16TL) could not pull down Lin28a (Fig. 4a). This was also confirmed by EMSA analysis of pre-microRNAs and anti Lin28a antibody (Fig. 4b). In EMSA pre-miR-9-1 as well as pre-let-7a-1 form several complexes with proteins from d0 P19 cell extracts. Formation of one of the complexes is abolished upon addition of anti Lin28a but not unspecific antibody (Fig. 4b). This suggests that Lin28a bound to pre-miR-9-1 and pre-let-7a-1 forms a complex with the anti Lin28a antibody, preventing the substrates to enter the gel. Alternatively, anti Lin28a antibody could be binding to Lin28a and precluding its association with its substrates. Importantly, pre-miR-16 was not shifted in undifferentiated cell extracts. This provides additional evidence for the specificity of Lin28a binding.

### The knockdown of Lin28a leads to increased levels of miR-9

Lin28a expression is dynamically regulated throughout neuronal differentiation[33]. Its expression is elevated at early stages of development and is switched off during differentiation. This regulation is essential for the inhibition of let-7 production at the early stages of differentiation and development and for maintaining pluripotency[33,35]. We observed a steady decrease in Lin28 until day 6 and a sharp drop in its expression on day 8 (Supplementary Fig. 1a). This decline coincided with a sharp increase in miR-9 levels on day 8 even though a substantial accumulation of primary miR-9 transcripts occurs at earlier stages of neuronal differentiation (Fig. 1a,b).

To determine whether Lin28a controls miR-9 levels, we transfected P19 cells with anti-Lin28a siRNAs. To initiate miR-9 expression, we then induced transfected cells to differentiate. Western blot analysis of Lin28a expression on day 4 of differentiation demonstrated that the protein was depleted to approximately 20-30% of control treatment (Fig. 5a). As expected, Lin28a depletion resulted in a 4-fold increase in let-7a levels (Fig. 5b). The level of miR-101 and miR-122, miRs unrelated to neuronal development, was unchanged. Crucially, Lin28a knockdown resulted in a modest but statistically significant 1.6-fold increase in miR-9 levels on day 4 of P19 neuronal differentiation (Fig. 5b).

To uncouple the effects of differentiation and control of miR-9 levels we performed pri-microRNA transgene overexpression in undifferentiated P19 cells. Overexpression of pri-miR-9 and pri-let-7a driven by a CMV promoter resulted in a very small induction of mature microRNAs (Supplementary Fig. 4). Importantly, overexpression of pri-let-7a-1/miR-16 TL mutant, which escapes Lin28a-medaited regulation, produced more than twenty fold more of

mature let-7a. This suggests that the accumulation of miR-9 and let-7a levels in undifferentiated cells is post-transcriptionally suppressed. Interestingly, overexpression of cognate pri-miR-9-1/miR-16 TL mutant did not result in de-repression of miR-9 accumulation (Supplementary Fig. 4). This implies the existence of additional layers of post-transcriptional miR-9 regulation, most likely preventing accumulation of mature microRNA in undifferentiated cells.

All these results suggest that Lin28a expression has an influence on the level of miR-9 *in vivo*. The difference between the observed effects of Lin28 depletion on the miR-9 and let-7 levels could be due to different levels of corresponding primary transcripts available at early stages of differentiation. The expression of the let-7 primary transcript is stable throughout differentiation, whereas the miR-9 primary transcript is not detected in undifferentiated P19 cells and only begins to accumulate during early stages of neuronal differentiation[17]. Together, these results provide evidence implicating Lin28a in the regulation of brain-specific miR-9 abundance during neuronal differentiation.

## Untagged Lin28a affects miR-9 and neuronal differentiation

Next, we wanted to determine whether prolonged expression of Lin28a during neuronal differentiation could affect the level of let-7a and miR-9. To test this hypothesis, P19 cells constitutively expressing untagged or GFP-tagged Lin28a together with the relevant control cell lines were subjected to retinoic acid-induced neuronal differentiation. Western blot analysis of untagged and GFP-tagged Lin28a confirmed their prolonged expression throughout P19 differentiation (Fig. 6a,b). During the differentiation of P19 cells constitutively expressing untagged Lin28a, we observed a significant reduction in the size of embryonic bodies (Fig. 6c,d). Surprisingly, P19 cells with stable Lin28a-GFP expression were phenotypically indistinguishable from control P19 cell lines. This result indicates that GFP-tagged Lin28a does not confer all of the functions of the wild type protein. Indeed, prolonged GFP-Lin28a expression during neuronal differentiation resulted in an approximate 4-fold decrease in let-7a compared with control cells but had no significant effect on the level of miR-9 (Fig. 6e).

Strikingly, constitutive expression of untagged Lin28a resulted in a significant reduction in the miR-9 and let-7a levels at the final stages of P19 cell neuronal differentiation (Fig. 6e). Similar results were obtained from two independent Lin28a integrations. The western blot of Lin28a on extracts from differentiated P19 FRT/Lin28a and P19 Lin28a/GFP cells revealed similar levels of GFP-tagged and untagged Lin28a (Supplementary Fig. 5). Thus, the observed phenotypic and functional differences arose from qualitative but not quantitative differences between tagged and untagged Lin28a. The level of primary miR-9 transcripts was also decreased in P19 cells constitutively expressing untagged Lin28a, corroborating the existence of a negative feedback loop between miR-9 and the REST complex, which controls miR-9 expression and is reciprocally controlled by miR-9 (Supplementary Fig. 6). Together, these are important observations for two reasons: they validate Lin28a as a regulator of miR-9 levels, and they suggest that GFP-tagged Lin28a could be functionally compromised. Finally, our results provide evidence that the mechanism of Lin28a-mediated microRNA biogenesis inhibition might be different for let-7 and miR-9.

## Pre-miR-9 is destabilized in early stages of differentiation

It is well documented that Lin28a inhibits members of the let-7 family at the early stages of differentiation and development through recruitment of TuT4 (or TuT7), which uridylates pre-let-7 and leads to its degradation by DIS3L2-mediated pre-let-7 degradation[30,31,36]. Our *in vivo* data suggest that Lin28a could inhibit miR-9 through a different mechanism, because untagged Lin28a impairs miR-9 and let-7 processing, whereas only let-7 is affected by expression of the GFP-tagged Lin28a.

To determine whether pre-miR-9 is regulated in a manner different from pre-let-7, we performed *in vitro* uridylation assays in P19 cell extracts from subsequent stages of neuronal differentiation. Pre-let-7a was efficiently uridylated in extracts derived from undifferentiated P19 cells (Fig. 7a). The intensity of the band corresponding to the uridylated form of pre-let-7a was reduced in reactions with extracts isolated from subsequent stages of neuronal differentiation (Fig. 7a). This reduction resulted in a small but significant increase in the stability of the pre-let-7a probe (Fig. 7c). In contrast, pre-miR-9 was not converted to a uridylated form but instead was significantly destabilized in extracts derived from undifferentiated P19 cells (Fig. 7a,c).

Significantly, incubation of pre-miR-9 with extracts derived from days 4, 6, and 9 resulted in its gradual stabilization by 2-, 4-, and 5-fold, respectively, which correlates with the period when Lin28a expression is reduced. Pre-miR-9-2 and pre-miR-9-3 are also destabilized in extract derived from d0 P19 cells (Supplementary Fig. 7). Importantly, pri-miR-9-1/miR-16 TL mutant, which does not bind Lin28a (Fig. 4a), is not destabilized in extracts from undifferentiated cells (Supplementary Fig. 7). Control pre-miR-101 and pre-let-7a probes were more stable under similar conditions (Fig. 7a,c). To establish how pre-miR-9 is degraded, we incubated 5′-end-labeled microRNA precursors in d0 extracts. Pre-miR-9-1 is more unstable than pre-let-7a and pre-miR-101, showing signs of 3′-5′ and 5′-3′ degradation (Fig. 7b,d). These results validate our *in vivo* data and point to different mechanisms by which miR-9 and let-7a levels are post-transcriptionally regulated during neuronal differentiation.

## Lin28a destabilizes pre-miR-9 by a uridylation-independent mechanism

Thus far we have shown that Lin28a can bind to the miR-9 CTL and influence miR-9 cellular levels. In addition, we have demonstrated that pre-miR-9 is rendered unstable in P19 cell extracts by a mechanism that is different than that for pre-let-7. To determine whether Lin28a mediates the observed destabilization of pre-miR-9 in undifferentiated cells, we performed pre-miR processing assays in P19 cell extracts with depleted Lin28a. Incubation of pre-let-7a with Lin28a-depleted extracts resulted in a reduction in pre-let-7a uridylation (Fig. 8a). The pre-miR-9 substrate was significantly stabilized in Lin28a-depleted extracts when compared with control (Fig. 8a,b). In similar conditions, the level of pre-miR-101 remained largely unchanged (Fig. 8a,b). Likewise, degradation of 5′-end labeled pre-miR-9-1 was strongly suppressed in Lin28a RNAi-depleted P19 d0 extracts compared with reactions in control RNAi extracts (Supplementary Fig. 8).

To further demonstrate the role of Lin28a in controlling pre-miR-9 stability we performed *in vitro* processing in extracts derived from cell lines with constitutive Lin28a expression. Similarly to wild type, d9 extracts derived from P19 cells stably expressing Lin28a-GFP support degradation of pre-miR-9-1 (Supplementary Fig. 9a,b). Pre-let-7a is uridylated in extracts from d0 and d9 derived from both P19 Lin28a-GFP and P19/FRT Lin28a cells. Notably, pre-miR-9-1 is not stabilized in d9 extracts derived from cells constitutively expressing GFP-tagged Lin28a (Supplementary Fig. 9a,b). These results further support the role of Lin28a in pre-miR-9 destabilization, which leads to decreased cellular levels of miR-9. Since *in vitro* processing reactions are uncoupled from the effects of transcription, the above results suggest that Lin28a can regulate pre-miR-9 post-transcriptionally.

### Induced Lin28a in differentiated cells downregulates miR-9

To test whether *in vivo* regulation of miR-9 by Lin28a is achievable after the cells have been differentiated we created Tet-On 3G P19 cells that express Lin28a under a doxycycline (Dox) inducible CMV promoter. Selected clones were subjected to RA-mediated differentiation and programmed with Dox at day 8 of differentiation, when the miR-9 levels approach maximum (Fig. 1). The cells were harvested at day 9 and compared with uninduced cells from the corresponding clones. One of the analyzed clones (P19 Tet-On 3G Lin28a 3#) showed induction of Lin28a upon Dox treatment (Fig. 9); albeit the levels were much lower when compared with undifferentiated cells. Crucially, only this clone, but not those which did not induce Lin28a, showed a specific downregulation of miR-9 and let-7a levels (Fig. 9b). The levels of pri-miR-9 transcripts were also decreased upon Dox treatment (Fig. 9b), suggesting that Lin28a can directly or indirectly influence the abundance of primary microRNA-9. Notably, pri-let-7a-1 levels were upregulated supporting the previously suggested role of Lin28a in repressing pri-let-7a-1 Drosha cleavage.

All our results support specific binding of Lin28a to the miR-9 CTL and its role in regulating cellular miR-9 levels. Our *in vitro* processing data strongly suggest that pre-miR-9 is regulated transcriptionally and post-transcriptionally by a Lin28a-mediated degradation mechanism. These results pave the way to further in-depth analysis required to determine the fine details of Lin28a-mediated control of miR-9, and towards better understanding of Lin28a contribution to neuronal function and differentiation.

## DISCUSSION

The biogenesis of microRNAs is a multi-step process that needs to be finely regulated, reflecting their many important roles in animal cells. Despite extensive research in the biological functions of microRNAs, little is known about the post-transcriptional mechanisms controlling their abundance. In many cases, the levels of primary microRNA transcripts are not correlated with the absolute levels of corresponding mature microRNAs[37]. In these cases, post-transcriptional regulation of microRNA processing is predicted to play a major role in controlling the level of the microRNAs in question[2,38,39]. For example, during neuronal differentiation, the let-7 levels are negatively correlated with the expression of Lin28 but display no correlation with its corresponding primary transcripts[40]. Similar observations have been made during the development of *C. elegans*[41].

Additionally, the biogenesis of brain-enriched miR-7, which is produced from a ubiquitous primary transcript, is inhibited by the HuR/MSI2 complex in non-neuronal cells[28]. Our current study shows that the levels of neuro-specific miR-9, which is responsible for neuronal development, undergo extensive transcriptional and post-transcriptional regulation.

miR-9 is transcriptionally suppressed by the anti-neural REST complex[17,18]. During neuronal differentiation, miR-9 target components of REST, allowing their own expression and that of other neuronal genes. Additionally, miR-9 promotes neural cell differentiation by targeting the TLX nuclear receptor, which is responsible for the maintenance of self-renewal[42]. In accordance with previous findings, we observed an increase in the level of miR-9 during RA-induced neuronal differentiation in P19 cells[43]. At the early stages of differentiation the accumulation of the three miR-9 primary transcripts substantially exceeded the accumulation of mature miR-9. These results point to the existence of previously uncharacterized post-transcriptional mechanisms regulating the intercellular levels of miR-9.

Using SILAC coupled with RNA pull-down and Mass Spectrometry[28], we identified several putative regulators of miR-9. We isolated Lin28a as a factor binding to the miR-9 CTL in undifferentiated P19 cells. It is believed that let-7 family members are the main microRNAs regulated by Lin28 during neuronal differentiation[44]. During muscle differentiation Lin28 and MBNL1 control miR-1 biogenesis through a uridylation-dependent mechanism[45]. An AGGAG consensus sequence was previously found to be crucial for the association between the Zn-knuckle domain (ZKD) of Lin28a and the let-7 CTL[46]. The miR-9 CTL has a GGAG motif, which can provide a platform for interaction with Lin28a. However, other U-rich sequences were shown to interact with Lin28a through its cold shock domain[29]. In accordance with these observations, pre-miR-9-1 and pre-miR-9-2 were shown to bind recombinant Lin28a *in vitro*[47]. Interestingly, several studies have used crosslinking and immunoprecipitation coupled with high-throughput sequencing (CLIP-seq) to identify targets for Lin28a binding but failed to detect miR-9 precursors[48,49]. These studies focused on undifferentiated embryonic stem cells and somatic cells. Therefore, it is plausible that such an approach could result in a failure to capture targets that are dynamically regulated throughout differentiation.

The constitutive expression of untagged Lin28a during neuronal differentiation resulted in a severe differentiation phenotype characterized by small embryonic bodies and reduced levels of mature miR-9 and let-7a. Previously, it has been reported that constitutive expression of Lin28-GFP inhibits let-7a processing in P19 cells and results in a neuronal phenotype that is independent of let-7[35]. Unexpectedly, constitutive expression of a Lin28a-GFP-tagged protein resulted in efficient reduction of let-7a but not miR-9 levels. Likewise, a severe differentiation phenotype was only evident in P19 cells constitutively expressing untagged but not GFP-tagged Lin28a protein. Notably, it has been shown that miR-9 depletion also results in a severe differentiation phenotype characterized by small embryonic bodies, which corroborates our results[50]. First, these findings suggest that decreased let-7 levels are not sufficient to induce an aberrant P19 differentiation phenotype. Second, the mechanisms for Lin28a-mediated inhibition of miR-9 and let-7 are different. Our *in vitro* processing results, obtained from the wild type cells and cells constitutively expressing

Lin28a, indicate that Lin28a destabilizes pre-miR-9 but does not induce uridylation as observed for pre-let-7 transcripts[30]. Furthermore, induction of Lin28a expression in differentiated cells leads to reduction of miR-9 levels, arguing that the Lin28a control over miR-9 is not restricted to differentiating cells. Further in-depth analysis is required to determine the effectors of the Lin28a-mediated control of pre-miR-9 stability and understand their contribution to neuronal differentiation.

miR-9 and miR-124 have been shown to be master regulators of neuronal programs because they alone can transform adult fibroblasts into neurons[22]. We hypothesize that their highly restricted, brain-specific expression profile needs to be safeguarded by several non-mutually exclusive mechanisms. Here, we show that miR-9 is transcriptionally and post-transcriptionally controlled. We present evidence that untagged Lin28a inhibits miR-9 processing by destabilizing pre-miR-9 through a uridylation-independent mechanism. This finding sheds more light on the role of Lin28a in neuronal differentiation. Altogether, our results demonstrate that transcriptionally regulated microRNAs can undergo complementary post-transcriptional control. This has important implications for the understanding of how microRNAs are regulated and the development of novel microRNA-based compounds and therapeutics.

## METHODS

### Cell culture and neuronal differentiation conditions

Mouse teratocarcinoma P19 cells or HeLa cells (ATCC) were maintained in standard DMEM medium (Life Technologies), supplemented with 10% foetal bovine serum (Life Technologies). All-trans Retinoic Acid (RA) (Sigma) was used to induce neuronal differentiation. Briefly, ~12×10$^6$ cells were plated on a non-adhesive dish in DMEM supplemented with 5% serum and supplemented with 1μM of RA. This induced the formation of embryonic bodies. After 4 days the embryonic bodies were re-suspended in DMEM supplemented with 10% serum and re-plated on an adhesive dish. Differentiation was followed up to 19 days post induction. At d9 cells displayed neuronal-like morphology. For SILAC Mass Spectrometry, undifferentiated cells were cultured in DMEM supplemented with "heavy" [$^{13}$C]Arg/[$^{13}$C]Lys isotopes and differentiation was performed using DMEM supplemented with "light" [$^{12}$C]Arg/[$^{12}$Lys] isotopes (Pierce SILAC Proteins Quantitation Kit – Thermo Scientific).

### Real time qRT-PCR and miRNA qRT-PCR analysis

Real time qRT–PCR was performed using the SuperScript III Platinum SYBR Green One-Step qRT-PCR Kit (Life Technologies) following the manufacturer's instructions on a Roche 480 LightCycler. Generally, 1 μl (500 ng) of total RNA isolated with TRIzol (Life Technologies) was used in a 20 μl reaction, and each sample was run in duplicate. To assess the levels of the corresponding transcripts, values were normalised to Cyclophilin A mRNA levels. For each measurement three independent experiments were performed. Primers are listed in Supplementary Table 4. MicroRNA qRT-PCR analysis was performed using the miSript qRT-PCR kit (Qiagen) on total RNA isolated with TRIzol (Life Technologies) and each sample was run in duplicate. To assess the levels of the corresponding microRNAs,

values were normalised to miR-16. For each measurement three independent experiments were performed.

## Northern blot analysis

20μg of total RNA was mixed with an equal volume of loading buffer (95% Formamide, 18mM EDTA, 0.025% SDS, Xylene Cyanol, Bromophenol blue) and resolved on a 10% PAGE-Urea gel. The ribosomal RNA was visualised with ethidium bromide to confirm equal loading. The RNA was transferred from the gel onto nitrocellulose membrane (Hybond N). The membrane was cross-linked twice with UV and pre-hybridised overnight at 40°C with 10mL of hybridisation buffer (1xSSC, 1%SDS, 200μg/mL ssDNA). A Northern probe was prepared using the *mir*Vana miR Probe Construction Kit (Life Technologies). In the first step a dsDNA template for T7 transcription was generated according to the manufacturer's instructions. The probe was denatured at 95°C for 1min, placed on ice and hybridised against the membrane for 2h at 40°C in 10mL of hybridisation buffer. Subsequently the membrane was washed 2-3 times for 30min each with 50mL of wash buffer (0.2%SSC, 0.2%SDS). The signal was registered with a radiographic film or exposed to a phosphoimaging screen and scanned on a FLA-5100 scanner (Fujifilm).

## Western blot analysis

Total protein samples (100μg per lane), isolated by sonication, were resolved by standard NuPAGE SDS-PAGE electrophoresis with MOPS running buffer (Life Technologies) and transferred onto nitrocellulose membrane. The membrane was blocked overnight at 4°C with 1:10 Western Blocking Reagent (Roche) in TBS buffer with 0.1% of Tween-20 (TBST). The following day the membrane was incubated for 1h at RT with primary antibody solution in 1:20 Western Blocking Reagent diluted in TBST: rabbit polyclonal anti Lin28a (A177) (1:1000, Cell Signalling Technology), rabbit polyclonal anti Msi1 (N3C3) (1:1000, GeneTex), rabbit monoclonal anti hnRNP A1 (1:1000, D21H11) (Cell Signalling Technology), Lin28b (1:1000, Cell Signalling Technology), Tuj1 (1:20,000, GeneTex), GFAP (1:1000, SIGMA), DHX9 (1:1000, Protein-Tech), mouse-monoclonal anti–β-tubulin (1:10,000, Sigma). After washing in TBST, the blots were incubated with the appropriate secondary antibodies conjugated to horseradish peroxidase and detected with SuperSignal West Pico detection reagent (Thermo Scientific). The membranes were stripped using ReBlot Plus Strong Antibody Stripping Solution (Chemicon) equilibrated in water, blocked in 1:10 western blocking solution in TBST and re-probed as described above. Full scans of the western blots presented in the manuscript are shown in the Supplementary Fig 10.

## *In vitro* processing assays

Pri-miRNA and pre-miRNA substrates were prepared by standard *in vitro* transcription with T7 RNA polymerase in the presence of [alpha-$^{32}$P]-UTP. Where indicated pre-miRNA probes were 5′end-labeled with [gamma-$^{32}$P]-ATP. The templates used to generate the transcripts were prepared by PCR amplification from cloned fragments of the human genome using corresponding primers (Supplementary Table 2). Pri-miR-9-1/miR-16 TL and pri-let-7a-1/miR-16 TL templates were prepared based on mutagenesis of the wild type pri-microRNA plasmids by replacing the terminal loops with the terminal loop from the miR-16

using corresponding primers (Supplementary Table 2). Gel purified probes ($50 \times 10^3$ c.p.m. (counts per minute), ~20 pmol) were incubated in 30 μl reaction mixtures containing 50% (v/v) total P19 cell extracts (appx. 10 μg/μl), 0.5 mM ATP, 20 mM creatine phosphate, 3.2 mM $MgCl_2$. Reactions were incubated at 37 °C for 30 min followed by phenol-chloroform extraction, precipitation, and 8% (w/v) denaturing gel electrophoresis. In the case of pre-miRNA processing 0.25 mM UTP was added to the reaction mixture. The signal was registered with a radiographic film or exposed to a phosphoimaging screen and scanned on a FLA-5100 scanner (Fujifilm).

### EMSA

Electrophoretic Mobility Shift Assays (EMSA) was performed with internally labelled pre-microRNA transcript and whole cell extracts. Gel purified probes ($50 \times 10^3$ c.p.m. (counts per minute), ~20 pmol) were incubated in 30 μl reaction mixtures containing 50% (v/v) total P19 cell extracts (appx. 10 μg/μl), 0.5 mM ATP, 20 mM creatine phosphate, 3.2 mM $MgCl_2$. Reactions were incubated at 4 °C for 1h followed by electrophoresis in 6% (w/v) non-denaturing gel. Where indicated antibodies were added to reactions mixtures (1:100) in order to generate super-shift. The signal was registered with a radiographic film or exposed to a phosphoimaging screen and scanned on a FLA-5100 scanner (Fujifilm).

### RNA pull down and Mass Spectrometry

RNA pull down and Mass Spectrometry were performed as described previously[28]. Briefly, total protein extracts from undifferentiated or differentiated P19 cells grown in "light" [$^{12}$C]Arg/[$^{12}$Lys] and "heavy" [$^{13}$C]Arg/[$^{13}$C]Lys isotopes, respectively, were incubated with synthesised RNAs, chemically coupled to agarose beads. All synthetic RNAs used are listed in Supplementary Table 3. The incubation was followed by a series of washes with Roeder D buffer (100mM KCl, 20% (v/v) glycerol, 0.2mM EDTA, 100mM Tris pH 8.0). After the final wash the beads with associated proteins were re-suspended in structure buffer (10mM Tris-HCl pH7.2, 1mM $MgCl_2$, 40mM NaCl) followed by treatment with RNAses. The samples were subsequently analysed by SDS-PAGE followed by Mass Spectrometry or Western Blot.

### RNAseq and small RNAseq

10μg of total RNA was isolated from d0 and d4 P19 cells and analysed on the Illumina HiSeq2000 platform. Sample processing and analysis were preformed by BGI genomics. Data visualisation was based on the bigwig files implemented into Ensembl Genome Browser.

### RNA interference and microRNA overexpression

Pools of siRNAs were obtained from Dharmacon in the format of three independent siRNAs targeting different regions of the mRNA coding for the protein of interest. Genomic fragment containing microRNAs were cloned in pCG T7 plasmid and transiently expressed in P19 cells. 4μg of siRNAs were delivered in two transfection events separated by 48h using nucleofection technology (AMAXA), according to manufacturer instructions. 2μg of PCG T7 plasmids expressing microRNAs were delivered using similar methodology. For

HeLa cells transfections were performed using Lipofectamine 2000 (Life Technologies), according to manufacturer instructions.

### Stable cell line generation

P19 cell lines with stable Lin28a-GFP or GFP only expression were gifts from Dr Eric Moss (The University of Medicine and Dentistry, New Jersey)[35]. Both lines were maintained in standard culture conditions. A P19 cell line expressing untagged Lin28a was developed using the Flp-in system (Life Technologies), according to manufacturer instructions. Briefly, the FRT site was randomly integrated in the genome and its integration was verified using Zeocin and lacZ selection markers. The Lin28a cDNA was integrated into the FRT site using Flp mediated recombination and the event was confirmed using hygromycin selection as well as Western blotting analysis. A P19 cell line with Tet-On 3G inducible expression of Lin28a was generated according to the manufactures instructions (Clontech Lab, Inc). Briefly, a pCMV-Tet3G plasmid coding for a Doxycycline (Dox)-responsive transactivator was integrated into undifferentiated P19 cells using a G418 selection marker. A pTRE3GBi-Luc plasmid expressing luciferase under a control transactivator-responsive promoter was used to select stable clones with high response to Dox (100ng/ml) treatment. Next, Lin28a was cloned to a pTRE3G-Bi plasmid and integrated into P19 cells with an active pCMV-Tet3G system using a linear Hygromycin selection marker. Selected clones were expanded and differentiated using Retinoic Acid, as described above. On day 8 of differentiation cells were induced with Dox (100ng/ml). The expression of Lin28a was checked at day 9 of differentiation.

## Supplementary Material

Refer to Web version on PubMed Central for supplementary material.

## ACKNOWLEDGEMENTS

## REFERENCES

1. Pasquinelli AE. NON-CODING RNA MicroRNAs and their targets: recognition, regulation and an emerging reciprocal relationship. Nature Reviews Genetics. 2012; 13:271–282.

2. Krol J, Loedige I, Filipowicz W. The widespread regulation of microRNA biogenesis, function and decay. Nat Rev Genet. 2010; 11:597–610. [PubMed: 20661255]

3. Wilson RC, Doudna JA. Molecular Mechanisms of RNA Interference. Annual Review of Biophysics. 2013; Vol 42:217–239. 42.

4. Hammond SM, Bernstein E, Beach D, Hannon GJ. An RNA-directed nuclease mediates post-transcriptional gene silencing in Drosophila cells. Nature. 2000; 404:293–6. [PubMed: 10749213]

5. Eulalio A, et al. Deadenylation is a widespread effect of miRNA regulation. RNA. 2009; 15:21–32. [PubMed: 19029310]

6. Fabian MR, Sonenberg N, Filipowicz W. Regulation of mRNA translation and stability by microRNAs. Annu Rev Biochem. 2010; 79:351–79. [PubMed: 20533884]

7. Landgraf P, et al. A mammalian microRNA expression atlas based on small RNA library sequencing. Cell. 2007; 129:1401–14. [PubMed: 17604727]

8. Farazi TA, Hoell JI, Morozov P, Tuschl T. MicroRNAs in human cancer. Adv Exp Med Biol. 2013; 774:1–20. [PubMed: 23377965]

9. Dimmeler S, Nicotera P. MicroRNAs in age-related diseases. EMBO Mol Med. 2013; 5:180–90. [PubMed: 23339066]

10. Thornton JE, Gregory RI. How does Lin28 let-7 control development and disease? Trends Cell Biol. 2012; 22:474–82. [PubMed: 22784697]

11. Bushati N, Cohen SM. MicroRNAs in neurodegeneration. Curr Opin Neurobiol. 2008; 18:292–6. [PubMed: 18662781]

12. Yates LA, Norbury CJ, Gilbert RJ. The long and short of microRNA. Cell. 2013; 153:516–9. [PubMed: 23622238]

13. Wang Z, et al. Transcriptional and epigenetic regulation of human microRNAs. Cancer Lett. 2013; 331:1–10. [PubMed: 23246373]

14. Cao X, Yeo G, Muotri AR, Kuwabara T, Gage FH. Noncoding RNAs in the mammalian central nervous system. Annu Rev Neurosci. 2006; 29:77–103. [PubMed: 16776580]

15. Krichevsky AM, Sonntag KC, Isacson O, Kosik KS. Specific microRNAs modulate embryonic stem cell-derived neurogenesis. Stem Cells. 2006; 24:857–64. [PubMed: 16357340]

16. Nowak JS, Michlewski G. miRNAs in development and pathogenesis of the nervous system. Biochemical Society Transactions. 2013; 41:815–820. [PubMed: 23863137]

17. Laneve P, et al. A minicircuitry involving REST and CREB controls miR-9-2 expression during human neuronal differentiation. Nucleic Acids Res. 2010; 38:6895–905. [PubMed: 20624818]

18. Conaco C, Otto S, Han JJ, Mandel G. Reciprocal actions of REST and a microRNA promote neuronal identity. Proc Natl Acad Sci U S A. 2006; 103:2422–7. [PubMed: 16461918]

19. Leucht C, et al. MicroRNA-9 directs late organizer activity of the midbrainhindbrain boundary. Nat Neurosci. 2008; 11:641–8. [PubMed: 18454145]

20. Wurst W, Bally-Cuif L. Neural plate patterning: upstream and downstream of the isthmic organizer. Nat Rev Neurosci. 2001; 2:99–108. [PubMed: 11253000]

21. Shibata M, Nakao H, Kiyonari H, Abe T, Aizawa S. MicroRNA-9 regulates neurogenesis in mouse telencephalon by targeting multiple transcription factors. J Neurosci. 2011; 31:3407–22. [PubMed: 21368052]

22. Yoo AS, et al. MicroRNA-mediated conversion of human fibroblasts to neurons. Nature. 2011; 476:228–31. [PubMed: 21753754]

23. Guil S, Caceres JF. The multifunctional RNA-binding protein hnRNP A1 is required for processing of miR-18a. Nat Struct Mol Biol. 2007; 14:591–6. [PubMed: 17558416]

24. Michlewski G, Guil S, Semple CA, Caceres JF. Posttranscriptional regulation of miRNAs harboring conserved terminal loops. Mol Cell. 2008; 32:383–93. [PubMed: 18995836]

25. Michlewski G, Caceres JF. Antagonistic role of hnRNP A1 and KSRP in the regulation of let-7a biogenesis. Nat Struct Mol Biol. 2010; 17:1011–8. [PubMed: 20639884]

26. Choudhury NR, Michlewski G. Terminal loop-mediated control of microRNA biogenesis. Biochemical Society Transactions. 2012; 40:789–793. [PubMed: 22817735]

27. Castilla-Llorente V, Nicastro G, Ramos A. Terminal loop-mediated regulation of miRNA biogenesis: selectivity and mechanisms. Biochem Soc Trans. 2013; 41:861–5. [PubMed: 23863145]

28. Choudhury NR, et al. Tissue-specific control of brain-enriched miR-7 biogenesis. Genes & Development. 2013; 27:24–38. [PubMed: 23307866]

29. Mayr F, Heinemann U. Mechanisms of Lin28-Mediated miRNA and mRNA Regulation-A Structural and Functional Perspective. Int J Mol Sci. 2013; 14:16532–53. [PubMed: 23939427]

30. Heo I, et al. TUT4 in concert with Lin28 suppresses microRNA biogenesis through pre-microRNA uridylation. Cell. 2009; 138:696–708. [PubMed: 19703396]

31. Chang HM, Triboulet R, Thornton JE, Gregory RI. A role for the Perlman syndrome exonuclease Dis3l2 in the Lin28-let-7 pathway. Nature. 2013; 497:244–8. [PubMed: 23594738]

32. Blahna MT, Hata A. Regulation of miRNA biogenesis as an integrated component of growth factor signaling. Curr Opin Cell Biol. 2013; 25:233–40. [PubMed: 23312066]

33. Viswanathan SR, Daley GQ, Gregory RI. Selective blockade of microRNA processing by Lin28. Science. 2008; 320:97–100. [PubMed: 18292307]

34. Trabucchi M, et al. The RNA-binding protein KSRP promotes the biogenesis of a subset of microRNAs. Nature. 2009; 459:1010–4. [PubMed: 19458619]

35. Balzer E, Heine C, Jiang Q, Lee VM, Moss EG. LIN28 alters cell fate succession and acts independently of the let-7 microRNA during neurogliogenesis in vitro. Development. 2010; 137:891–900. [PubMed: 20179095]

36. Thornton JE, Chang HM, Piskounova E, Gregory RI. Lin28-mediated control of let-7 microRNA expression by alternative TUTases Zcchc11 (TUT4) and Zcchc6 (TUT7). RNA. 2012; 18:1875–85. [PubMed: 22898984]

37. Van Wynsberghe PM, et al. LIN-28 co-transcriptionally binds primary let-7 to regulate miRNA maturation in Caenorhabditis elegans. Nat Struct Mol Biol. 2011; 18:302–8. [PubMed: 21297634]

38. Kim VN, Han J, Siomi MC. Biogenesis of small RNAs in animals. Nat Rev Mol Cell Biol. 2009; 10:126–39. [PubMed: 19165215]

39. Siomi H, Siomi MC. Posttranscriptional regulation of microRNA biogenesis in animals. Mol Cell. 2010; 38:323–32. [PubMed: 20471939]

40. Rybak A, et al. A feedback loop comprising lin-28 and let-7 controls pre-let-7 maturation during neural stem-cell commitment. Nat Cell Biol. 2008; 10:987–93. [PubMed: 18604195]

41. Kai ZS, Finnegan EF, Huang S, Pasquinelli AE. Multiple cis-elements and trans-acting factors regulate dynamic spatio-temporal transcription of let-7 in Caenorhabditis elegans. Developmental Biology. 2013; 374:223–233. [PubMed: 23201578]

42. Zhao C, Sun G, Li S, Shi Y. A feedback regulatory loop involving microRNA-9 and nuclear receptor TLX in neural stem cell fate determination. Nat Struct Mol Biol. 2009; 16:365–71. [PubMed: 19330006]

43. Sempere LF, et al. Expression profiling of mammalian microRNAs uncovers a subset of brain-expressed microRNAs with possible roles in murine and human neuronal differentiation. Genome Biol. 2004; 5:R13. [PubMed: 15003116]

44. Wulczyn FG, et al. Post-transcriptional regulation of the let-7 microRNA during neural cell specification. FASEB J. 2007; 21:415–26. [PubMed: 17167072]

45. Rau F, et al. Misregulation of miR-1 processing is associated with heart defects in myotonic dystrophy. Nat Struct Mol Biol. 2011; 18:840–5. [PubMed: 21685920]

46. Nam Y, Chen C, Gregory RI, Chou JJ, Sliz P. Molecular basis for interaction of let-7 microRNAs with Lin28. Cell. 2011; 147:1080–91. [PubMed: 22078496]

47. Towbin H, et al. Systematic screens of proteins binding to synthetic microRNA precursors. Nucleic Acids Res. 2013; 41:e47. [PubMed: 23221640]

48. Cho J, et al. LIN28A is a suppressor of ER-associated translation in embryonic stem cells. Cell. 2012; 151:765–77. [PubMed: 23102813]

49. Wilbert ML, et al. LIN28 binds messenger RNAs at GGAGA motifs and regulates splicing factor abundance. Mol Cell. 2012; 48:195–206. [PubMed: 22959275]

50. Delaloy C, et al. MicroRNA-9 coordinates proliferation and migration of human embryonic stem cell-derived neural progenitors. Cell Stem Cell. 2010; 6:323–35. [PubMed: 20362537]

**a**


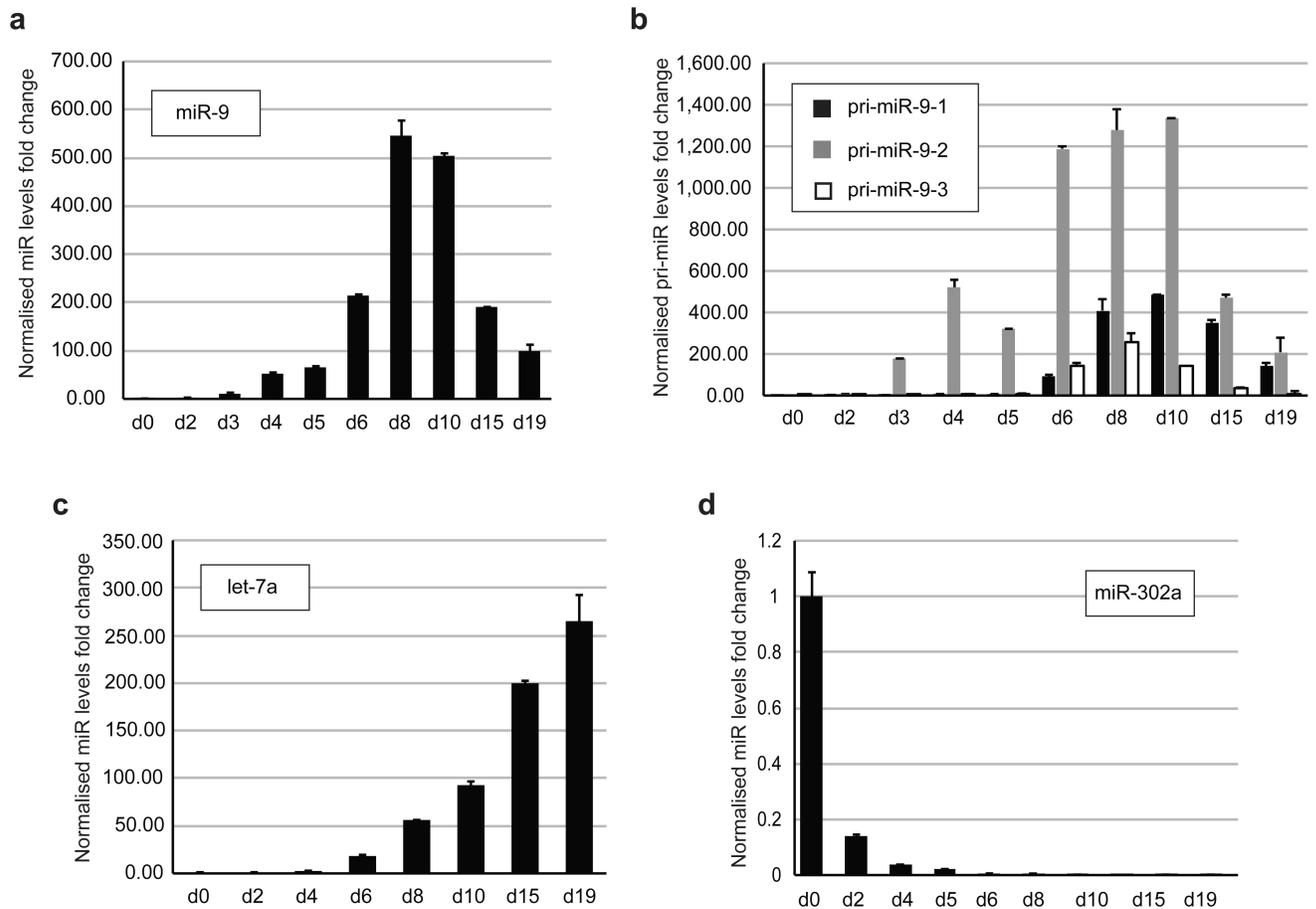
**b**



**c**



**d**



**Figure 1. The level of brain-specific miR-9 is transcriptionally and post-transcriptionally regulated during RA-induced neuronal differentiation of P19 cells**

(**a, c, d**) Real-time qRT-PCR analysis of mature miR-9, let-7a and miR-302a levels at different stages of RA-induced neuronal differentiation (Day – d). The values were normalized to miR-16 levels. The fold change was plotted relative to values derived from undifferentiated cells (d0), which were set to 1. Mean values and standard deviations (SD) of three independent biological replicates are shown. (**b**) Real-time qRT–PCR of miR-9 primary transcripts (pri-miR) at different stages of RA-induced P19 cell neuronal differentiation. The fold changes of the corresponding pri-miRNA abundance, pri-miR-9-1 (black bars), pri-miR-9-2 (grey bars) and pri-miR-9-3 (white bars), were plotted relative to the d0 values, which were set to 1. The values were normalized to the cyclophilin A mRNA levels. Mean values and standard deviations (SD) of three independent experiments are shown.
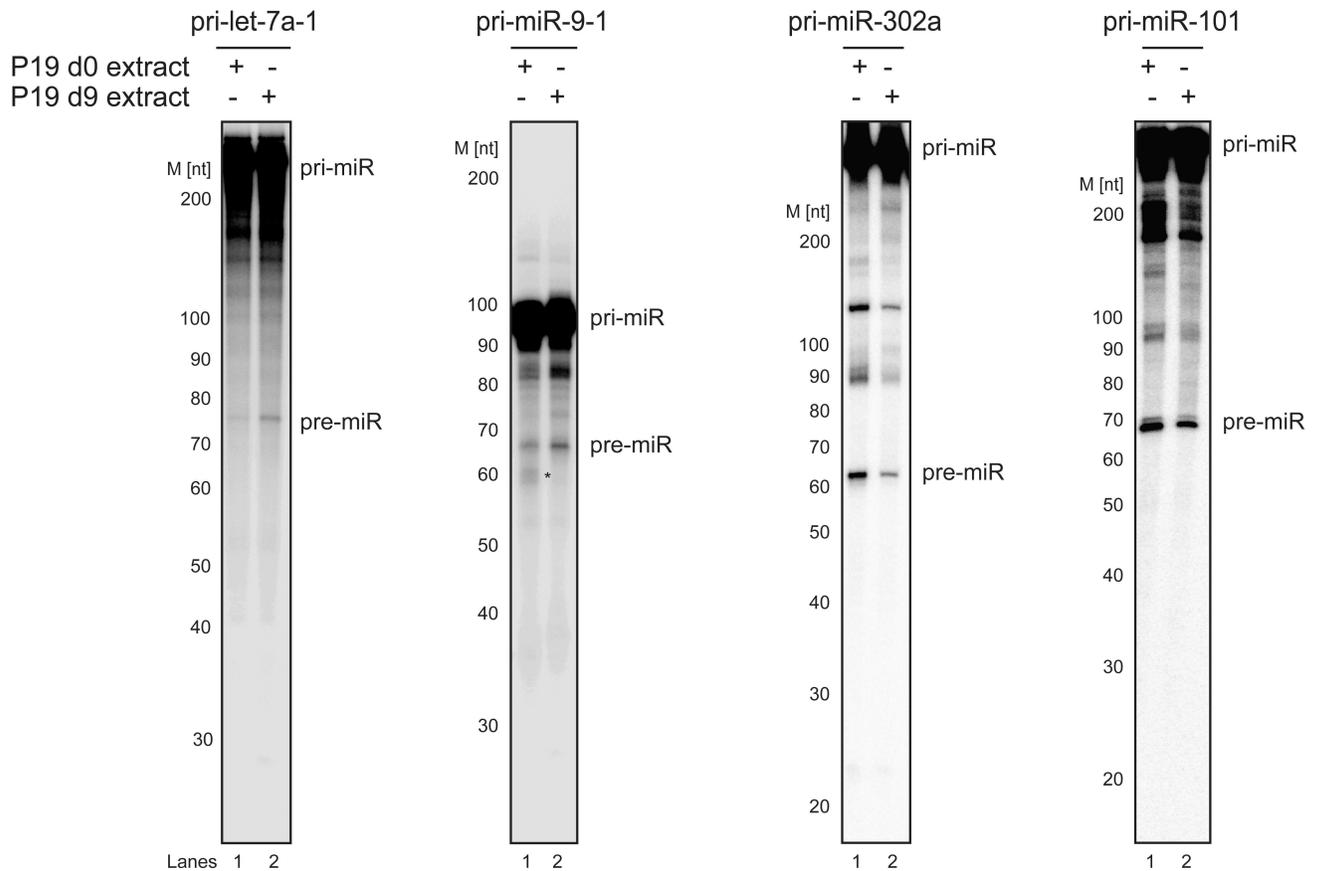
**Figure 2. Let-7a, miR-9 and miR-302a primary transcripts are differentially processed in undifferentiated and differentiated extracts from P19 cells**

Internally radiolabeled primary transcripts ($50 \times 10^3$ c.p.m. (counts per minute), approximately 20 pmol) were incubated in the presence of either d0 (Lanes 1) or d9 (Lanes 2) P19 cell extracts. The products were analyzed on an 8% denaturing polyacrylamide gel. [M] – RNA size marker. (*) – Nonspecific *in vitro* processing products. Pri-miR-101 processing served as a control. The results are representative of at least three independent experiments.
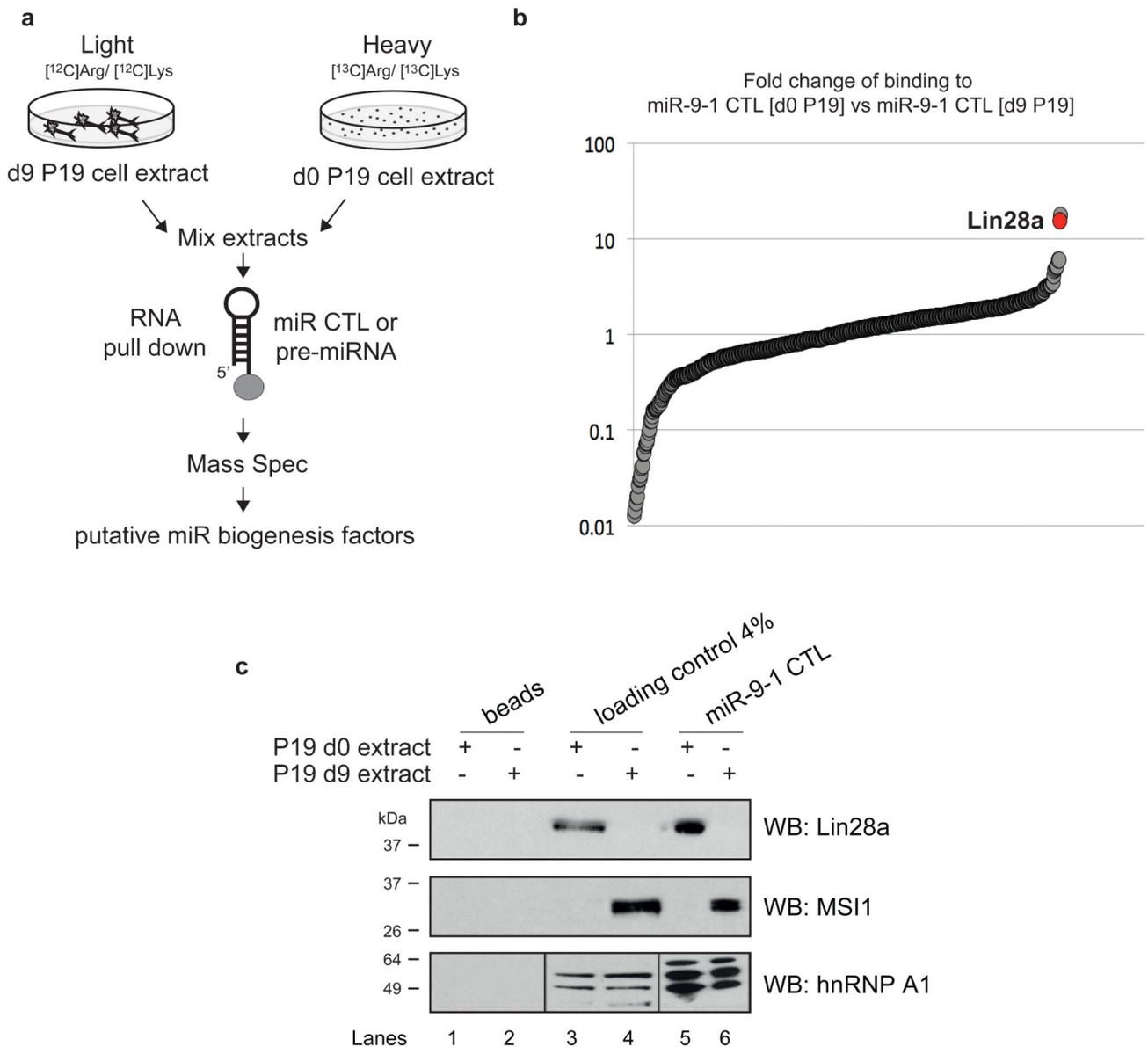
**Figure 3. SILAC combined with RNA pull-down and Mass Spectrometry reveals putative regulators of brain-specific microRNA biogenesis**

(**a**) Schematic of the method. P19 cells were grown in "light" medium containing $^{12}C6$-arginine and $^{12}C6$-lysine or "heavy" medium containing $^{13}C6$-arginine and $^{13}C6$-lysine. Cells grown in "light" medium were subjected to retinoic acid-induced neuronal differentiation until d9. Next, RNA pull-down was performed with agarose beads covalently linked to microRNA CTLs or pre-microRNAs and incubated with premixed extracts from "light" d9 or "heavy" d0 P19 cells. After RNase treatment, the supernatants were subjected to quantitative mass spectrometry, which identifies putative microRNA biogenesis factors. (**b**) The graph represents the fold enrichment of proteins that bind to the miR-9-1 CTL in experiments with "heavy" d0 P19 cell extracts compared with "light" d9 P19 cell extracts. The values are presented on a log10 scale. The Lin28a protein is indicated in red. (**c**)

Western blot analysis of miR-9-1 CTL RNA pull-down with d0 and d9 P19 cell extracts for Lin28a, MSI1 and hnRNP A1. Lanes 1 and 2 show reactions with beads alone and d0 and d9 cell extracts, respectively. Lanes 2 and 3 represent 4% (100 μg) of the loading control for d0 and d9 cell extracts, respectively. Lanes 5 and 6 represent miR-9-1 CTL RNA pull-downs with d0 and d9 cell extracts, respectively. Lanes 7 and 8 represent miR-9-1 CTL RNA pull-downs with d0 and d9 cell extracts, respectively. The results are representative of at least three independent experiments.
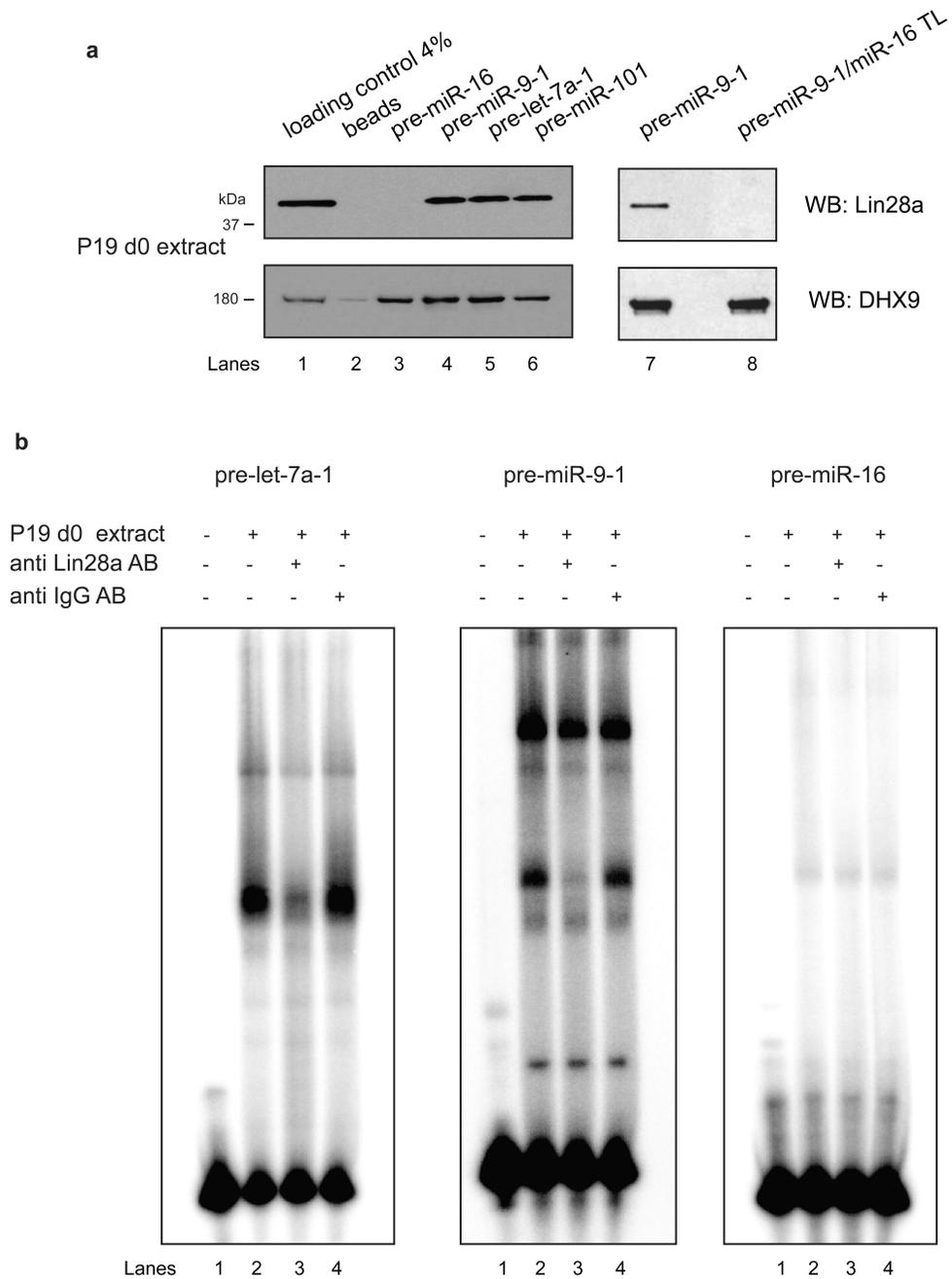
**a**



**b**



**Figure 4. Lin28a binds specifically to pre-microRNAs**

(**a**) Western blot analysis of pre-microRNA pull-down with d0 P19 cell extracts for Lin28a and DHX9. Lane 1 represents 4% (100 μg) of the loading control. Lane 2 shows reactions with beads alone, lane 3 with pre-miR-16, lanes 4 and 7 with pre-miR-9-1, lane 5 with pre-let-7a-1, lane 6 with pre-miR-101 and lane 8 with pre-miR-9-1/miR-16 TL mutant. (**b**) EMSA analysis of pre-microRNAs in extracts from d0 P19 cells. Where indicated 1:100 of antibody was added to reaction mixture. Lane 1 represents controls without added extract, lane 2 with d0 extracts, lane 3 with d0 extract and anti Lin28a antibody and lane 4 with d0

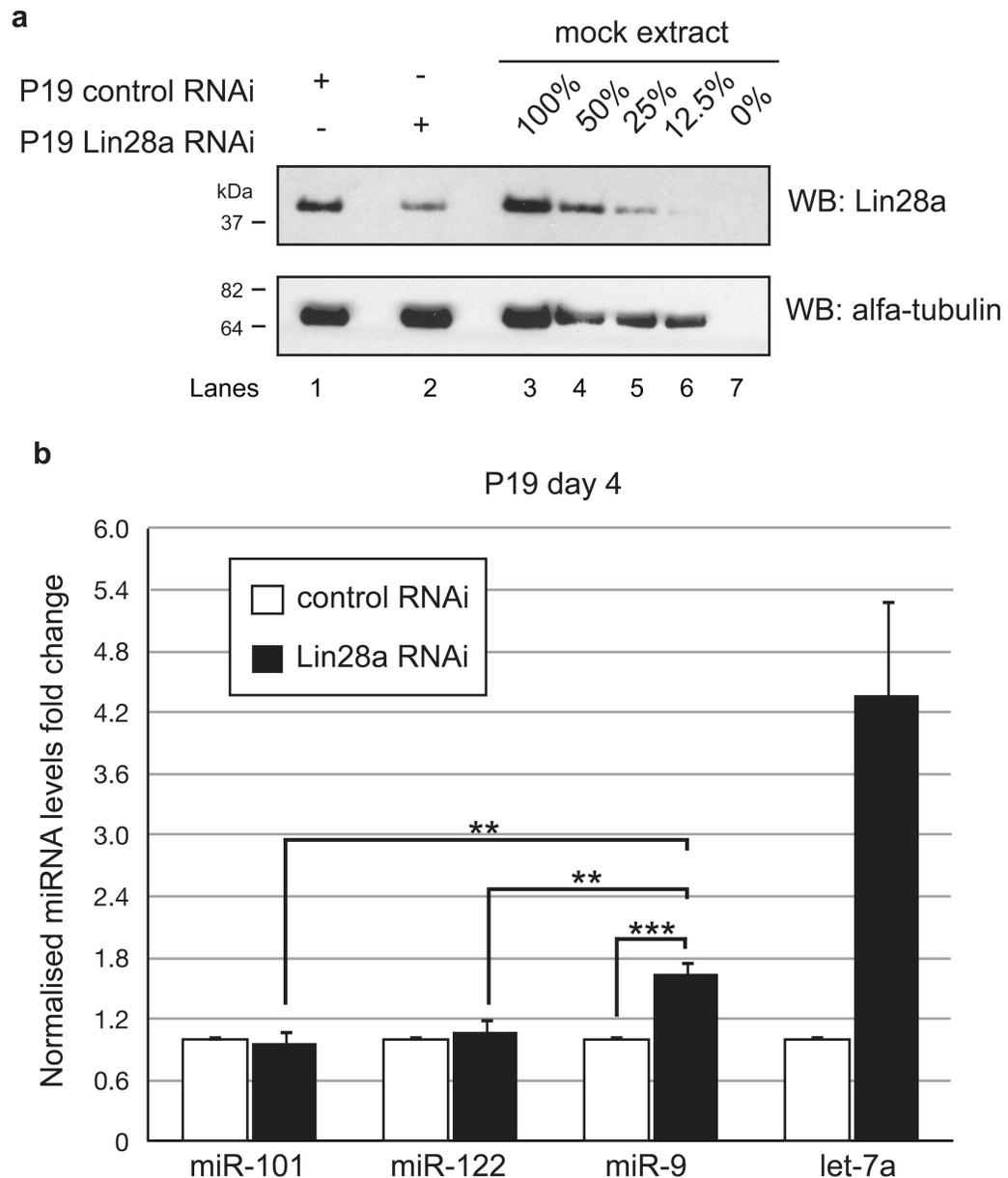and anti IgG antibody. The results are representative of at least three independent experiments.

**a**



**b**



**Figure 5. Lin28a regulates miR-9 levels differentiating P19 cells**

(**a**) Western blot analysis of protein extracts from mock-depleted P19 cells (Lane 1) and Lin28a-depleted P19 cells (Lane 2). Lanes 3 through 7 show serial dilutions of total protein extracts from mock-depleted P19 cells, providing an estimation of the linearity of the Western blot assay and the limit of detection. (**b**) Real-time qRT-PCR analysis of the mature miR-101, miR-122, miR-9 and let-7a levels on day 4 (d4) of RA-induced neuronal differentiation. The results from the mock-depleted cells are shown as white bars; the results from Lin28a-depleted cells are shown as black bars. The values were normalized to the miR-16 level. The fold change was plotted relative to values derived from mock-depleted cells, which were set to 1. Mean values and standard deviations (SD) of three independent

biological replicates are shown. Statistical significance was calculated using $t$-test (**) $-P$ 0.01, (***) $-P$ 0.001.
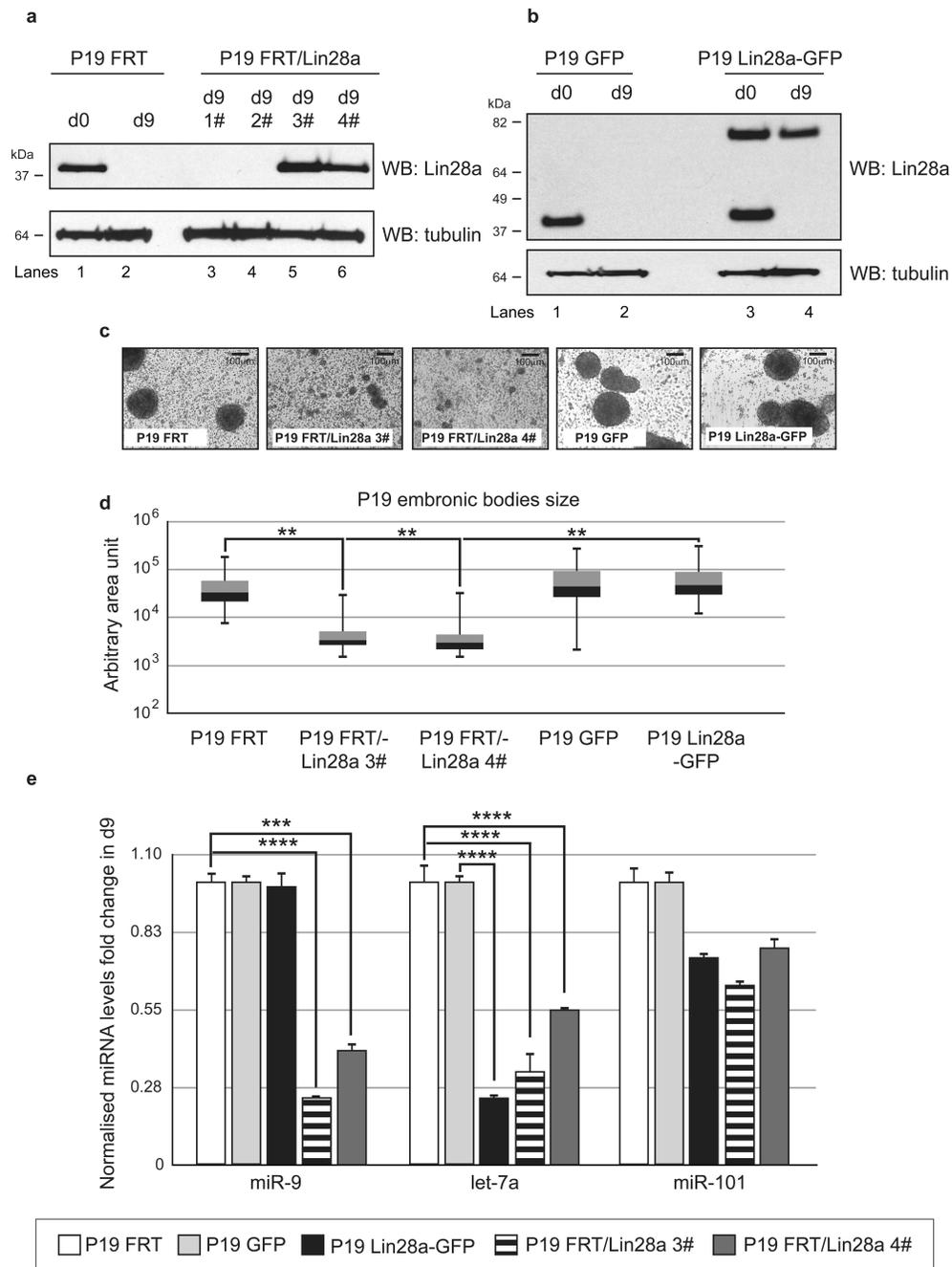
**Figure 6. Constitutive expression of untagged but not GFP-tagged Lin28a affects miR-9 biogenesis during P19 cell differentiation**

(**a**) Western blot analysis of Lin28a levels in P19 stable cell lines expressing untagged human Lin28a. Lanes 1 and 2 include d0 and d9 P19 cells with an integrated FRT site, respectively. Lanes 3 and 4 show the P19 FRT/Lin28a clone, which does not express Lin28a at day 9. Lanes 5 and 6 include P19 FRT/Lin28a clones with stable Lin28a expression in differentiated cells. Tubulin served as a loading control. (**b**) Western blot analysis of the Lin28a levels in P19 stable cell lines expressing GFP-tagged human Lin28a. Lanes 1 and 2 are d0 and d9 P19 cells with integrated GFP, respectively. Lanes 3 and 4 are P19 Lin28a-

GFP cell lines with stable expression of GFP-tagged human Lin28a in undifferentiated and differentiated cells, respectively. Tubulin served as a loading control. (**c**) Bright-field microscopy images showing representative images of P19 embryonic bodies at day 4 of differentiation. (**d**) Quantification of P19 embryonic bodies sizes at day 4 of differentiation represented as box plots. Statistical significance was calculated using the Mann-Whitney *U*-test (\*\*) - P 0.01, (\*\*\*) - P 0.001. (**e**) Real-time qRT-PCR analysis of mature miR-9, let-7a and miR-101 on day 9 of P19 FRT (white bars), P19 GFP (light grey bars), P19 GFP-Lin28a (black bars), P19 FRT/Lin28a 3# (horizontal lines bars) and P19 FRT/Lin28a 4# (dark grey bars). The values were normalized to miR-16 levels. The fold change was plotted relative to values derived from the corresponding control cell lines P19 FRT and P19 GFP, which were set to 1. Mean values and standard deviations (SD) of three independent biological replicates are shown. Statistical significance was calculated using *t*-test (\*\*\*) –P 0.001, (\*\*\*\*) - P 0.0001.
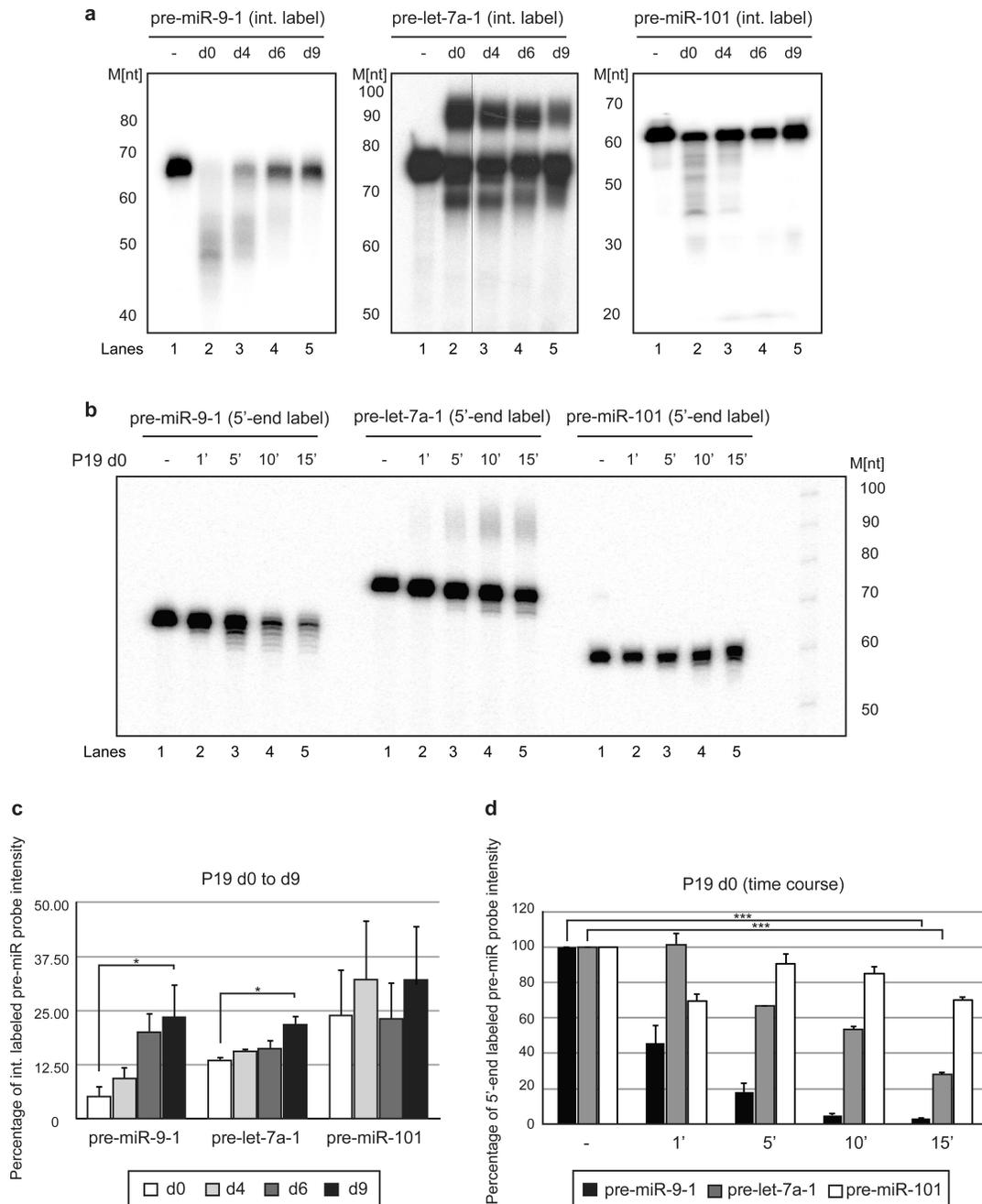
**Figure 7. Pre-miR-9 is destabilized in P19 cell extracts from the early stages of neuronal differentiation**

(**a**) *In vitro* processing assays were performed with internally radiolabeled pre-miR transcripts ($50 \times 10^3$ c.p.m. (counts per minute), approximately 20 pmol) in the presence of d0 (Lanes 2), d4 (Lanes 3), d6 (Lanes 4) or d9 (Lanes 4) P19 cell extracts. (-) represents an untreated control. Reactions were supplemented with 0.25 mM UTP. The products were analyzed on an 8% denaturing polyacrylamide gel. [M] - RNA size marker. (**b**) *In vitro* processing assays were performed with 5′-end labeled pre-miR transcripts ($50 \times 10^3$ c.p.m. (counts per minute), approximately 20 pmol). Pre-microRNAs were incubated in d0 P19 cell

extracts for 1 (1′), 5 (5′), 10 (10′) or 15 min (15′). The control (-) was incubated without extract for 15′. [M] - RNA size marker. (**c**) The percentage of pre-microRNA substrate intensity remaining after corresponding *in vitro* processing reactions was plotted relative to the control reactions set to 100. Mean values and standard deviations (SD) of three independent experiments are shown. Statistical significance was calculated using a *t*-test (*) –P   0.05, (***) –P   0.001.
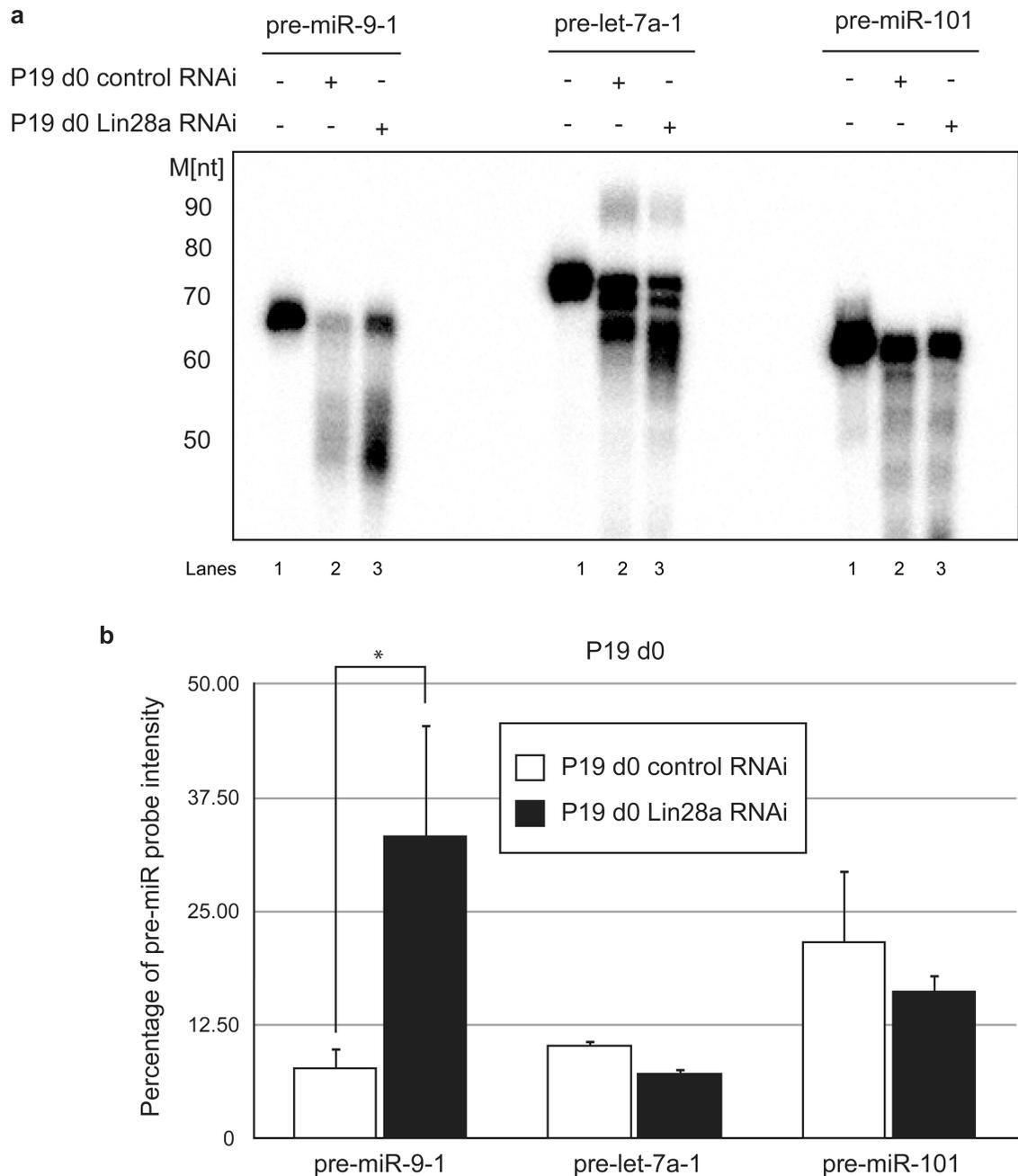
**a**



**b**



**Figure 8. Pre-miR-9 is stabilized in Lin28a-depleted P19 cell extracts**

*In vitro* processing assays were performed with internally radiolabeled pre-miR transcripts ($50 \times 10^3$ c.p.m. (counts per minute), approximately 20 pmol) in the presence of either mock-depleted (Lanes 2,5,8) or Lin28a-depleted (Lanes 3, 6, 9) d0 P19 cell extracts. (-) represents the untreated control (Lanes 1,4,7). Reactions were supplemented with 0.25 mM UTP. The products were analyzed on an 8% denaturing polyacrylamide gel. (**b**) The percentage of pre-microRNA substrate intensity remaining after corresponding *in vitro* processing reactions was plotted relative to the control reactions set to 100. Mean values and

standard deviations (SD) of three experimental replicates are shown. Statistical significance was calculated using a *t*-test (*) −P 0.05.
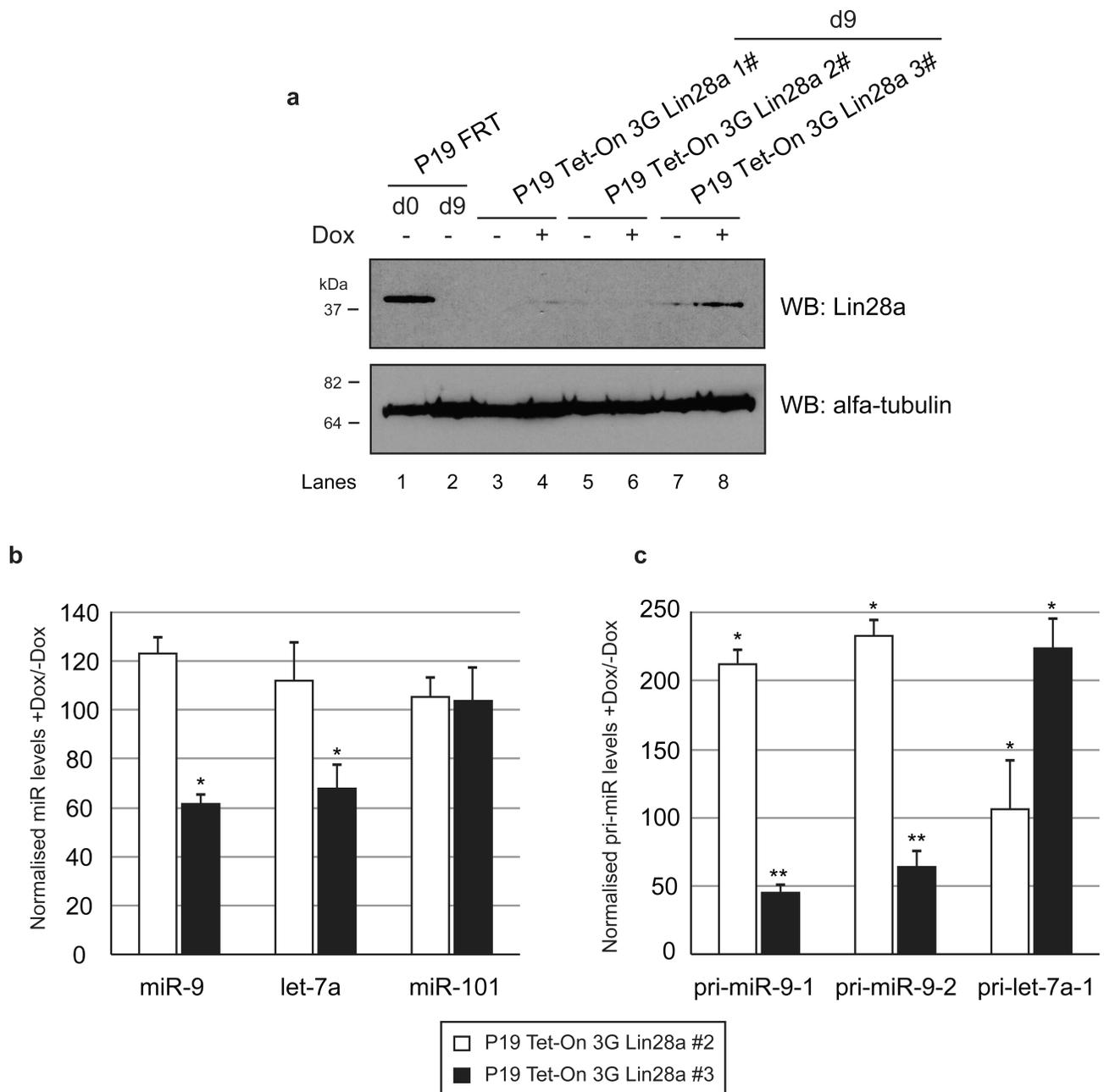
**a**



**Figure 9. Lin28a induction in differentiated P19 cells results in reduction of miR-9 levels.**
(**a**) Western blot analysis of protein extracts from control P19 cells (Lane 1 – d0 and Lane 2 – d9) and d9 of three colonies of P19 Tet-On 3G Lin28a cells. Lanes 3, 5 and 7 represent results from the corresponding cell lines without Dox. Lanes 4, 6 and 8 show results from the corresponding cell lines induced with Dox (100ng/ml). (**b**) Real-time qRT-PCR analysis of mature miR-9, let-7a and miR-101 levels of Dox-induced cells after RA-mediated neuronal differentiation. The results from P19 Tet-On 3G Lin28a #2, which failed to induce Lin28a, is shown as white bars; the results from P19 Tet-On 3G Lin28a #3, which induced Lin28a, are shown as black bars. The values were normalized to miR-16 levels. The fold

change was plotted relative to values derived from -Dox cells, which were set to 100. Mean values and standard deviations (SD) of three independent biological replicates are shown. Statistical significance was calculated using *t*-test (*) –P 0.05. (**c**) Real-time qRT-PCR analysis of the primary miR-9-1, miR-9-2 and let-7a-1 of Dox-induced cells after RA-mediated neuronal differentiation. The results from P19 Tet-On 3G Lin28a #2, which failed to induce Lin28a, is shown as white bars; the results from P19 Tet-On 3G Lin28a #3, which induced Lin28a, are shown as black bars. The values were normalized to cyclophilin A mRNA levels. Mean values and standard deviations (SD) of three independent experiments are shown (*) –P 0.05, (**) –P 0.01.